Journal of
Data Acquisition and Processing
ISSN: 1004-9037
https://sjcjycl.cn/
DOI: 10.5281/zenodo.7922998

A COMPACT CIRCULARLY POLARISED BROADBAND SQUARE RING MONOPOLE ANTENNA FOR WLAN AND WIMAX APPLICATIONS

Kranthi Kumar Andhe* and Dr. S Narayana Reddy
Department of E.C.E., Sri Venkateswara University,
Tirupati, Andhra Pradesh, India-517502
E-mail: kk.svu18@gmail.com, snreddysvu@yahoo.com

Abstract:
The development of simple and inexpensive broadband antennas for various applications has played a significant role in modern wireless communication systems, attracting academics to pursue further research and investigation. Antennas have become an indispensable component of wireless communication systems front ends. In this research work, a circularly polarized (CP) asymmetrical square ring monopole antenna with the amended ground plane is designed. An asymmetrical square ring patch plus an altered ground plane will make up the CP antenna. In the broadband antenna, symmetrical step-type ground stubs are used to achieve CP. The Axial Ratio Bandwidth (ARBW) of this antenna is 1.66 GHz (3.82– 5.48 GHz), while the impedance bandwidth (IBW) is 2.39 GHz (3.95– 6.34 GHz). The FR4 dielectric is used to develop and build the CP broadband antenna, which has a miniature dimension of 25 x 25 x 1.6 mm^3 and a peak gain of 3.3 dBic. The results of the tests are very similar to those of the simulations.

Keywords: Circular Polarization, Compact Size, Broadband, Impedance Bandwidth, Axial Ratio Bandwidth.

1. Introduction

The creation of low-profile broad CP planar antennas was necessitated by the growing demand for high-speed communication [1]. With CP antennas, polarisation mismatch, multipath fading, bad weather, Faraday rotation, selective plane absorptions, and reflections are less common. CP antennas provide additional options for putting transmitter and receiver because they do not have to match polarisation [2]. As a result, CP antennas outperform linear polarised antennas in data transfer. Recognizing this, several efforts have been undertaken to date, using various methodologies, to construct planar antennas that benefit both circular polarisation and broadband nature.

In [3], a chirp-shaped monopole radiator with asymmetric feed, slit-loaded patches produced broadband CP [4], [5]. In [6], CP is achieved by a C-shaped branch extending from the vertical monopole with a square ring slot on the ground plane. A crossed dipole in an octagonal ring [7], Substrate integrated waveguide with closed ring slot [8], monopole with rectangular slot, and metasurface of modified S-shape [9] produced CP. In[10]–[12], A parasitic metallic plate-based square patch antenna with corners pruned, a simple parasitic patch with dipole a crossed dipole antenna, loop feeding with driven patches, and parasitic patches generated CP. Using sequential phase rotation technique CP is generated in [13]–[15].

In this work, a compact 25 x 25 mm^2 square ring monopole antenna with the step-type etched ground plane is proposed for WLAN and WiMAX applications. Broad IBW and good CP radiation characteristics were achieved by using asymmetrical square ring monopole, and step type etched ground. To illustrate the correctness of this CP slot antenna, typical simulations were run and compared to measurements of the constructed prototype.

2. Antenna design

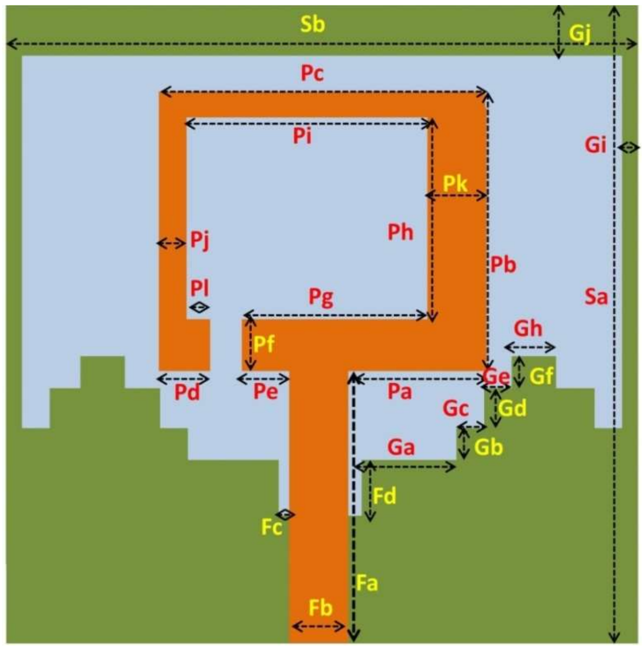

Fig.1: Antenna Structure

Figure 1 depicts the planned wideband CP antenna's architecture. The structure contains an asymmetrical rectangular ring patch monopole with the slot. The ground structure contains symmetrical step types on both sides of the feed line to enhance the ARBW. The dimensions of the proposed structure are shown in Table 1. The structure contains dielectric material of FR-4 substrate with height 1.6 mm, and the overall dimensions are 25 x 25 x 1.6 mm^3 is simulated and fabricated.

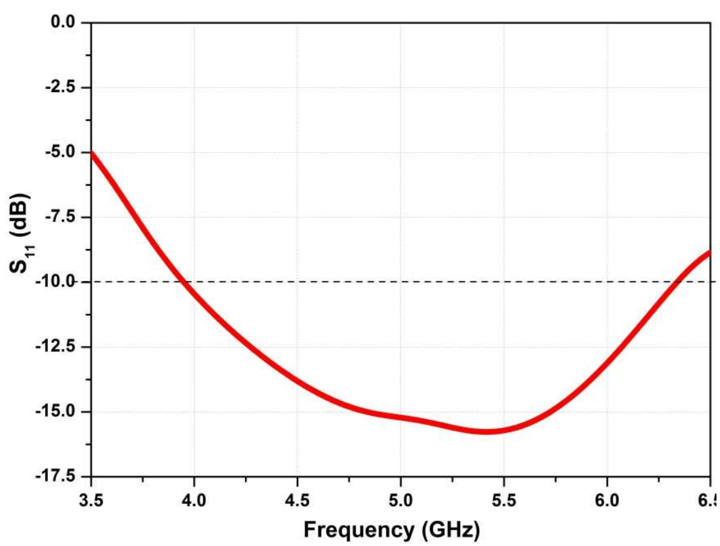

Fig. 2 Return loss

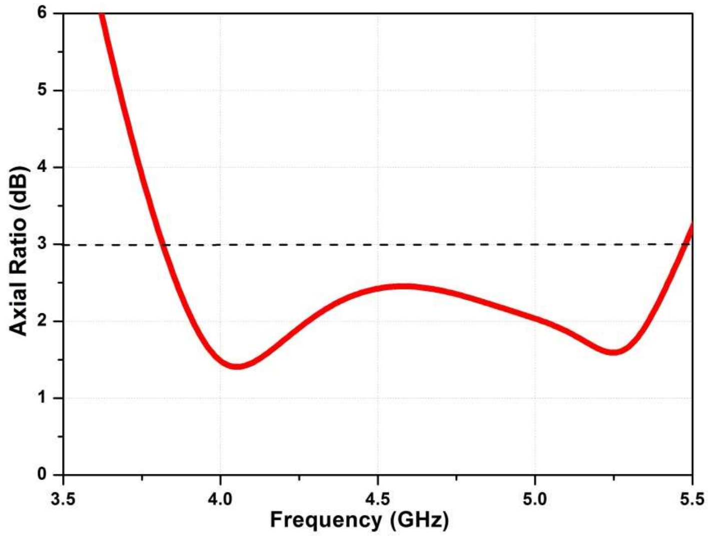

Fig. 3: Axial ratio

The return loss plot is shown in Fig.2. The frequency range of 3.95 GHz to 6.34 GHz is below the acceptable range of S11. The CP characteristics are shown in Fig.3, as the acceptable range is from 3.82 GHz to 5.48 GHz by covering both WLAN and WiMAX applications. Fig. 4(a) and Fig. 4(b) show the surface current distribution at 4.52 GHz and 5.24 GHz.

Table 1: Antenna Dimensions

Parameter	Sa	Sb	Ga	Gb	Gc	Gd	Ge	Gf	Gh
Units(mm)	25	25	3.5	1	1	1.5	1.25	1.5	2.5
Parameter	Gi	Gj	Fa	Fb	Fc	Fd	Pa	Pb	Pc
Units(mm)	0.5	2	9.5	2.4	0.3	2	4.8	12	12
Parameter	Pd	Pe	Pf	Pg	Ph	Pi	Pj	Pk	pl
Units(mm)	2.5	1.05	2	6.25	9	9	1	1.25	1.5

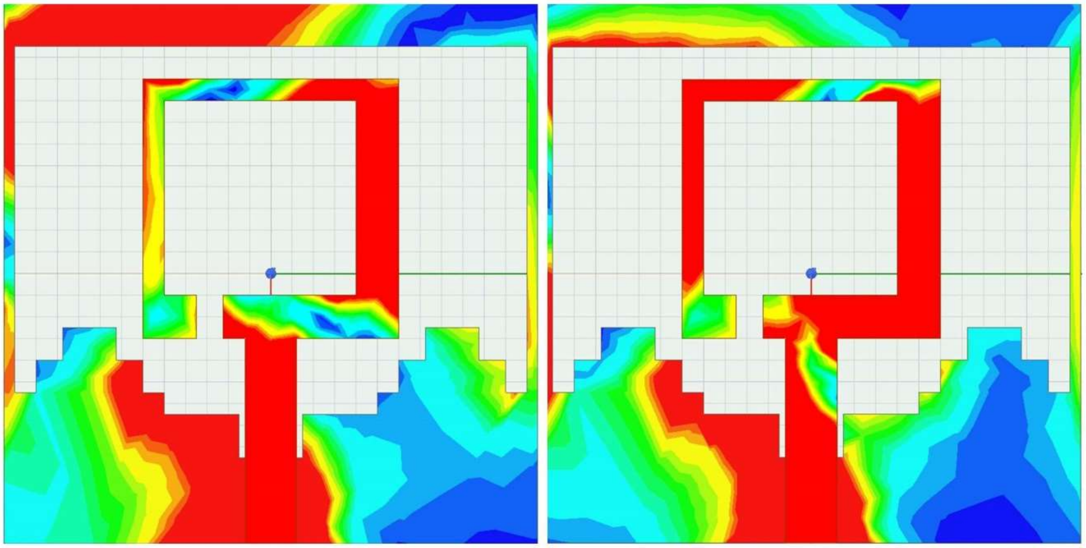

(a) (b)

Fig. 4 Surface current distribution at (a) 4.52 GHz (b) 5.24GHz

3. Circular Polarization Mechanism

The electric field vector representation is used to observe the CP mechanism as shown in Fig. 5 and Fig. 6 from the +z direction (top view). Fig. 5 shows the CP mechanism at 4.24 GHz at various phases of 0^0, 90^0, $180^{0,}$ and 270^0. Fig. 6 shows the CP mechanism at 5.24 GHz at various phases of 0^0, 90^0, $180^{0,}$ and 270^0, the trace on phase 0^0, 90^0, $180^{0,}$ and 270^0 shows the circularly polarized behavior. It rotates in the clockwise direction from the +Z direction, causing LHCP.

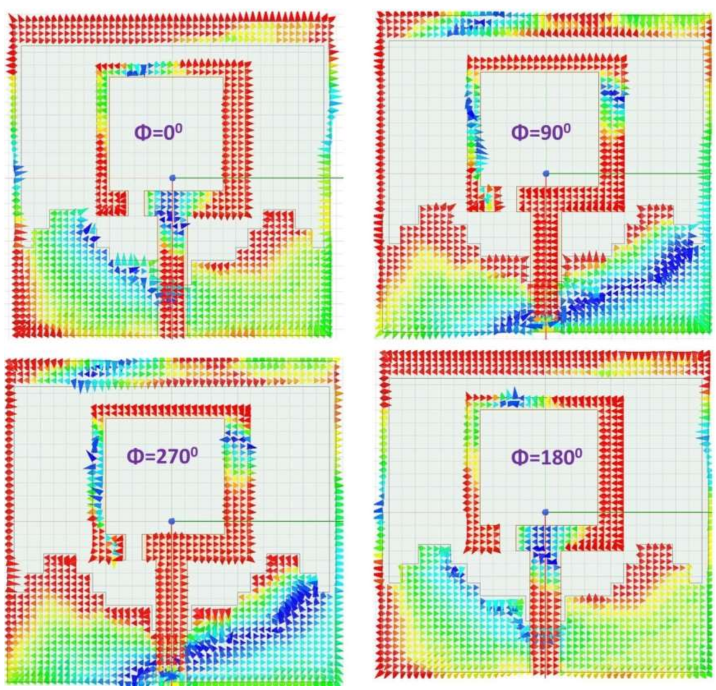

Fig 5: Circular polarization mechanism at various instances of phase at 4.24 GHz

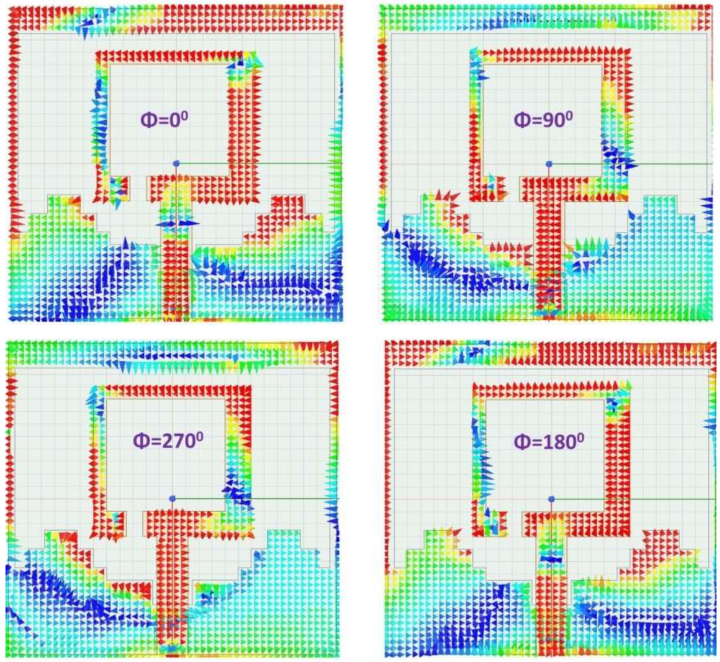

Fig 6: Circular polarization mechanism at various instances of phase at 5.24 GHz

4. Experimental results

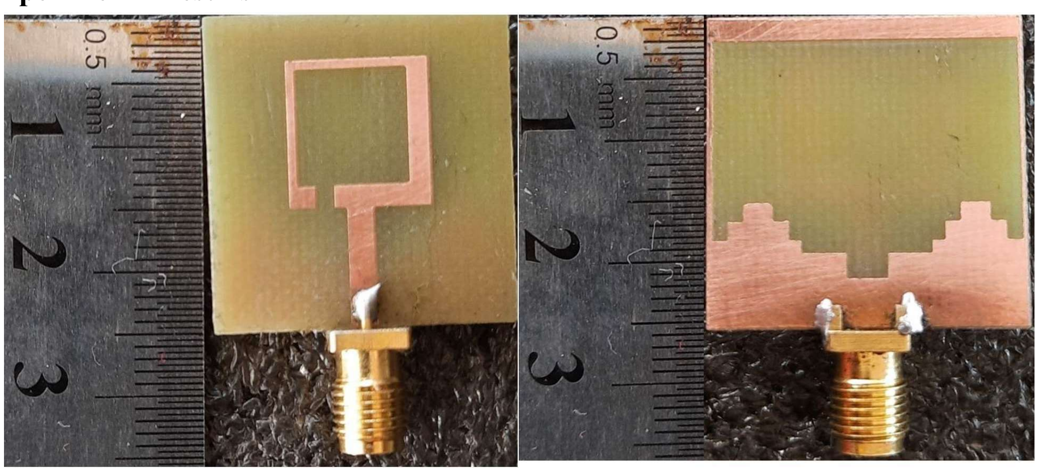

(a) (b)

Fig. 7 Fabricated prototype antenna (a) top view (b) bottom view

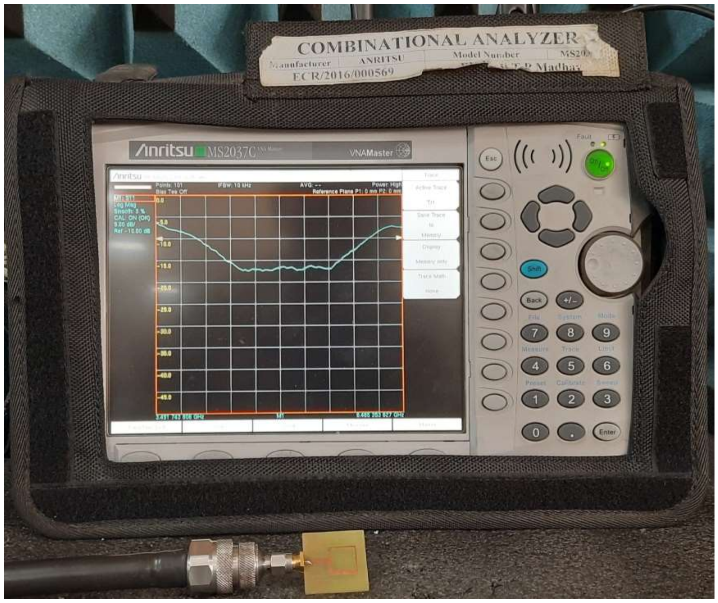

Fig. 8 Return loss measurement of fabricated prototype antenna

A prototype is built and tested to demonstrate the practicality of the proposed broadband CP antenna. The top view photograph is shown in Fig. 7(a), and the back view is shown in Fig. 7(b). Fig. 8 shows the measurement of the return loss of the prototype antenna. Fig. 9 shows the measurement of VSWR of the prototype antenna. The observed results suggest that the measured bandwidth is approximately 42.31 percent centered at 5.01 GHz (3.95–6.07 GHz), while the simulation is 46.45 percent (3.95–6.34 GHz), as shown in Fig. 10. Fig. 11 shows the simulated and measured comparative plots of VSWR charts.

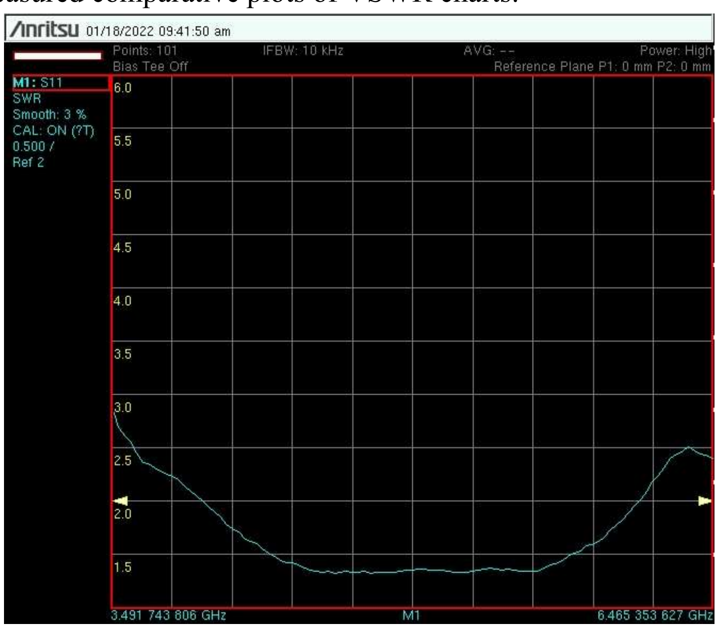

Fig. 9 VSWR measurement of fabricated prototype antenna

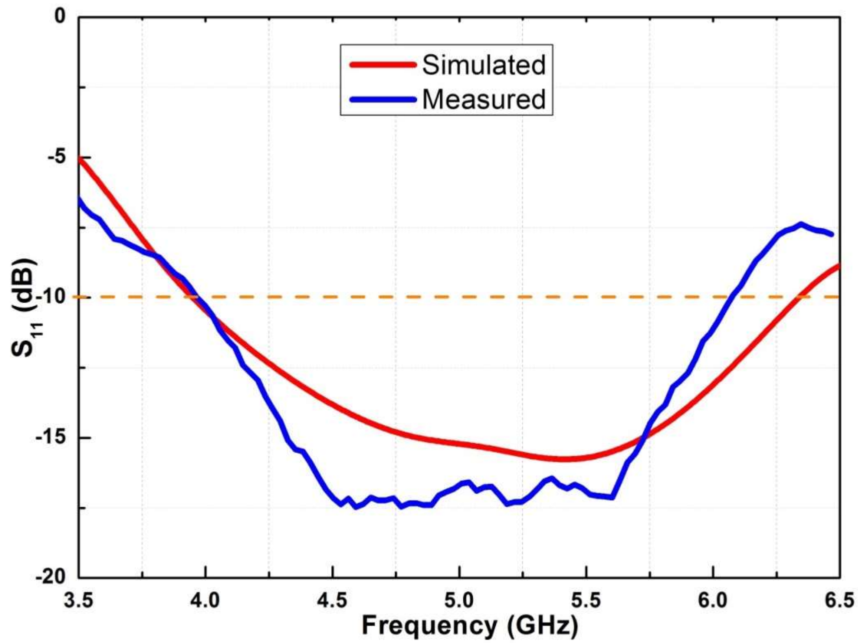

Fig. 10: Comparison result of return loss

The axial ratio charts are shown in Fig.12. The frequency extends from 3.95 to 5.45 GHz, with 31.91 percent centered at 4.7 GHz, according to the results. The simulated results range from 3.82 to 5.48 GHz, with 4.65 GHz accounting for 35.69 percent. The measured and simulated gains are about 3 dBic, as in Fig.13. The simulated and measured findings are reasonably consistent, with the minor variations attributable primarily to fabrication tolerance and welded joints.

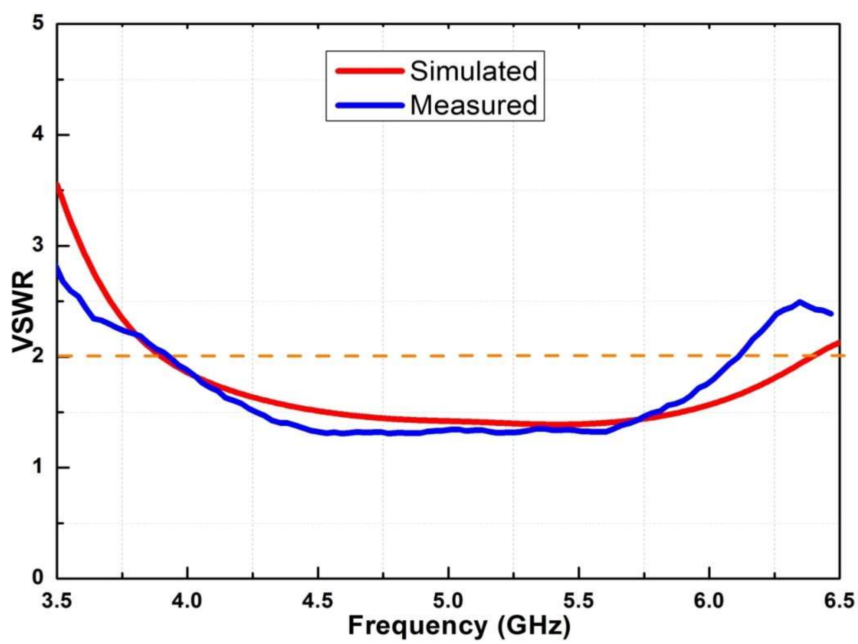

Fig 11: Comparison result of VSWR

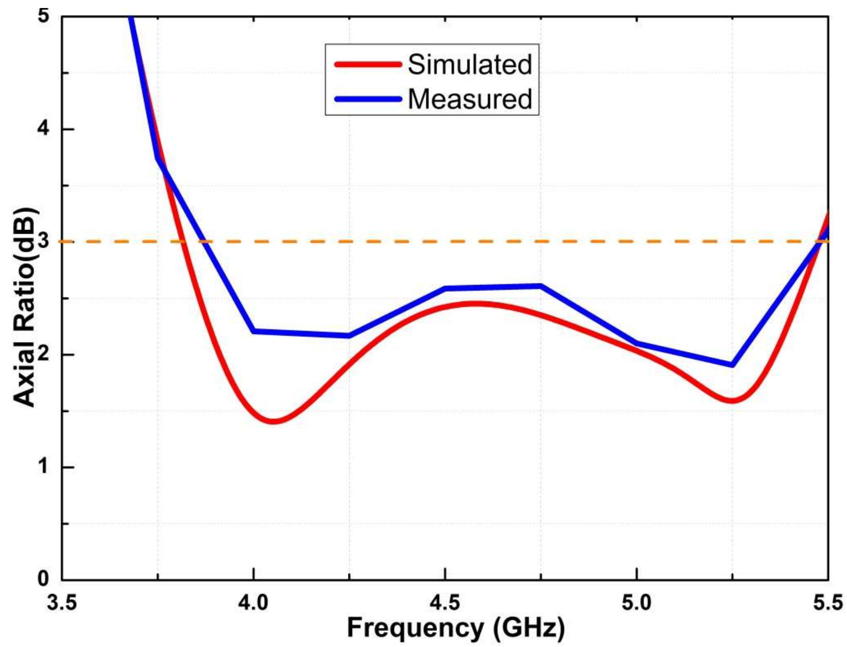

Fig 12: Comparison result of Axial Ratio

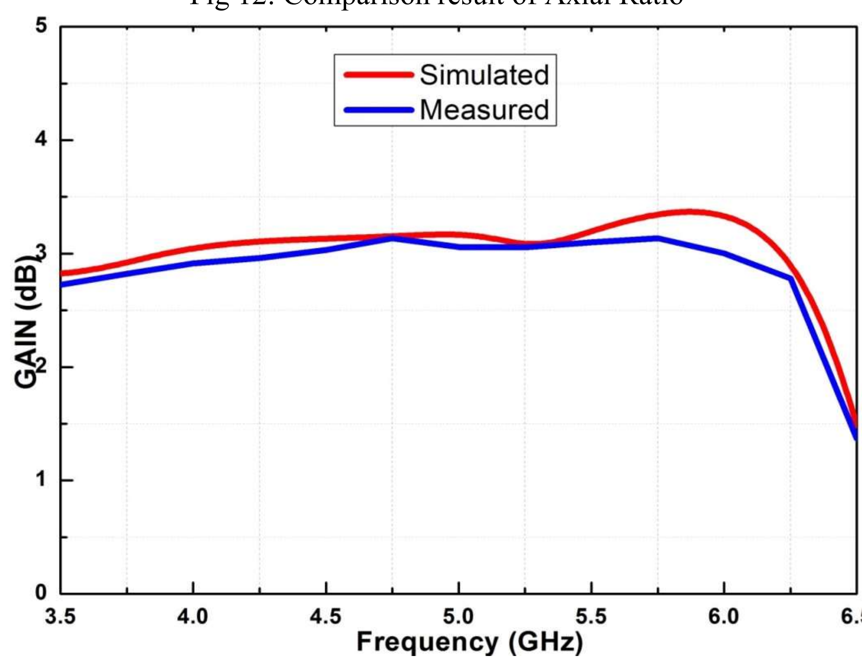

Fig 13: Comparison result of gain

Table 2. Comparison of the antenna's performance to published works

Ref.	**Impedance Band (GHz)**	**Circularly Polarized Band (GHz)**	**Dimensions (mm x mm)**
3	4.56 - 8.5	4.75 - 8.45	40 x 40
4	1.5 - 3.3	1.98 - 3.02	63 x 58
5	2 – 2.75	2.1 – 2.65	55 x 55

6	1.96 – 3.8	2.3 – 2.490	50 x 50
7	2.11 – 6.42	2.65 – 3.18	40 x 40
8	3.0 - 5.2	3.0 - 5.2	200 x 200
9	2.545- 2.685	2.58- 2.64	24.8 x 22
10	4.05 - 6.6	5.3 - 6.6	34 x 34
11	5.08 - 5.92	5.08 - 5.92	31 x 32
13	5.13 – 6.24	5.38 – 6.12	50 x 50
14	5.01 – 5.87	5.08 – 5.72	80 x 80
15	5.20 – 6.23	5.25 – 5.95	75 x 75
Proposed	**3.95 – 6.34**	**3.82 – 5.48**	**25 x 25**

Table 2 compares the proposed antenna's performance to various previously published designs. The proposed antenna has the smallest size among the reported antennas, as shown in the table. In addition, given the size of the suggested antenna, the impedance and ARBW is sufficient.

5. Conclusion

An asymmetrical square ring patch plus an altered ground plane is designed to make up the CP antenna. Symmetrical step-type ground stubs are used to achieve CP. The radiation features of the antenna return loss, VSWR, axial ratio, and gain are verified through a prototype of the antenna. ARBW of this antenna was 35.69 %, return loss has 46.45 %. A standard gain of 3.1 dBic was achieved throughout the bandwidth. This antenna is compatible with WLAN and WiMAX applications.

References:

[1] C. A. Balanis, *Antenna Theory: Analysis and Design*, 4th ed.: John Wiley & Sons, Inc, 2016. John wiley & sons, 2015.

[2] Steven (Shichang) Gao, Qi Luo and Fuguo Zhu, *Circularly Polarized Antennas*, 1st ed.: John Wiley & Sons, Ltd, 2013.

[3] H. Zhang, Y.-C. Jiao, L. Lu, and C. Zhang, “Broadband circularly polarized square-ring-loaded slot antenna with flat gains,” *IEEE Antennas Wirel. Propag. Lett.*, vol. 16, pp. 29–32, 2016.

[4] R.-C. Han and S.-S. Zhong, “Broadband circularly-polarised chifre-shaped monopole antenna with asymmetric feed,” *Electron. Lett.*, vol. 52, no. 4, pp. 256–258, 2016.

[5] Q. Chen, H. Zhang, L.-C. Yang, and T. Zhong, “A metasurface-based slit-loaded wideband circularly polarized crossed dipole antenna,” *Int. J. RF Microw. Comput. Eng.*, vol. 28, no. 1, p. e21173, 2018.

[6] C.-Y.-D. Sim, H.-D. Chen, L. Zuo, and T.-A. Chen, “CPW-fed square ring slot antenna with circular polarization radiation for WiMAX/WLAN applications,” *Microw. Opt. Technol. Lett.*, vol. 57, no. 4, pp. 886–891, 2015.

[7] J. Zhang and Z. Shen, "Dual-band shared-aperture UHF/UWB RFID reader antenna of circular polarization," *IEEE Trans. Antennas Propag.*, vol. 66, no. 8, pp. 3886–3893, 2018, doi: 10.1109/TAP.2018.2839883.

[8] C. Zhou, G. Wang, Y. Wang, B. Zong, and J. Ma, "CPW-fed dual-band linearly and circularly polarized antenna employing novel composite right/left-handed transmission-line," *IEEE Antennas Wirel. Propag. Lett.*, vol. 12, pp. 1073–1076, 2013.

[9] N. Supreeyatitikul, T. Lertwiriyaprapa, and C. Phongcharoenpanich, "S-shaped metasurface-based wideband circularly polarized patch antenna for C-Band applications," *IEEE Access*, vol. 9, pp. 23944–23955, 2021.

[10] H. H. Tran, N. Hussain, and T. T. Le, "Low-profile wideband circularly polarized MIMO antenna with polarization diversity for WLAN applications," *AEU-International J. Electron. Commun.*, vol. 108, pp. 172–180, 2019.

[11] H. H. Tran, I. Park, and T. K. Nguyen, "Circularly polarized bandwidth-enhanced crossed dipole antenna with a simple single parasitic element," *IEEE Antennas Wirel. Propag. Lett.*, vol. 16, pp. 1776–1779, 2017.

[12] K. Ding, C. Gao, D. Qu, and Q. Yin, "Compact broadband circularly polarized antenna with parasitic patches," *IEEE Trans. Antennas Propag.*, vol. 65, no. 9, pp. 4854–4857, 2017.

[13] K. Ding, C. Gao, T. Yu, D. Qu, and B. Zhang, "Gain-improved broadband circularly polarized antenna array with parasitic patches," *IEEE Antennas Wirel. Propag. Lett.*, vol. 16, pp. 1468–1471, 2016.

[14] C. Deng, Y. Li, Z. Zhang, and Z. Feng, "A wideband sequential-phase fed circularly polarized patch array," *IEEE Trans. Antennas Propag.*, vol. 62, no. 7, pp. 3890–3893, 2014.

[15] M. S. Ibrahim, H. Attia, Q. Cheng, and A. Mahmoud, "Wideband circularly polarized aperture coupled DRA array with sequential-phase feed at X-band," *Alexandria Eng. J.*, vol. 59, no. 6, pp. 4901–4908, 2020.